Turkish Journal of Physics

http://journals.tubitak.gov.tr/physics/

Research Article

Turk J Phys
(2014) 38: 228 – 237
© TÜBİTAK
doi:10.3906/fiz-1401-3

Annealing effect on zinc nanoferrite particles synthesized by spray pyrolysis of polymer precursor

Jessyamma KURIAN[1], **Subin JOHN**[2], **Jacob MATHEW**[2,*]
[1]Department of Physics, Bishop Abraham Memorial College, Thurithicad, India
[2]Department of Physics, Saint Berchmans College, Changanassery, India

Received: 10.01.2014 • **Accepted:** 08.05.2014 • **Published Online:** 11.06.2014 • **Printed:** 10.07.2014

Abstract: Nanosized zinc ferrite particles, prepared by spray pyrolysis method, were investigated by X-ray diffraction, transmission electron microscopy, energy dispersive spectroscopy, Fe^{57} Mossbauer spectroscopy, and vibrating sample magnetometer. The cubic crystalline phases were identified in all samples. The lattice parameter (a = 8.446 Å) and the average particle size of all the samples were determined. The particle sizes increased as the annealing temperature increased from 250 °C to 550 °C. The variation in structural parameters and particle size estimated from X-ray diffraction patterns of heat-treated samples suggested that the synthesized sample was in a 'metastable' state or a compositionally constrained state. The Mossbauer spectra of the annealed samples showed a single doublet, thereby indicating the presence of superparamagnetism. Magnetic studies using vibrating sample magnetometer also confirm the superparamagnetic nature of the material.

Key words: Nano zinc ferrites, spray pyrolysis, superparamagnetism

1. Introduction

Magnetic nanomaterials are an important class of functional materials, possessing unique magnetic properties, due to their small size. Researchers are synthesizing nanoforms of almost all kinds of magnetic materials by various methods to understand their physical properties, and particularly their electrical and magnetic properties [1]. Among them, spray pyrolysis is a promising method to produce particles with controlled morphology and very small particle size [2]. The spray-drying method of polymer precursors with appropriate metal nitrates is a simple and economic method that can be used to prepare numerous kinds of functional materials in nanoform [3]. In this paper, we report the synthesis of $ZnFe_2O_4$, a member of the magnetic spinel ferrites, using spray drying of a polymer precursor containing metal nitrates and its characterization using various techniques [2].

2. Experimental

2.1. Synthesis

R-grade ferric nitrate $Fe(NO_3)_3.6H_2O$, zinc nitrate $Zn(NO_3)_2.6H_2O$, and polyvinyl alcohol (PVA) with molecular weight of 125,000 in deionized water were used for making the precursor for the spray drying. Aqueous solutions of salts with different molar ratios of zinc nitrate and ferric nitrate were used. The presence of PVA helps the homogeneous distribution of the metal ions in the polymeric network structure and inhibits their

*Correspondence: jacob.chrisdale@gmail.com

segregation from the solution. The resulting viscous mixture of PVA and metal nitrates was spray dried at about 130 °C to obtain a black fluffy powder. A series of 5 such samples were prepared by spray technique with varying molar ratios of zinc nitrate and iron nitrate for understanding the effect of iron concentration on the formation of single-phase nano zinc ferrite nanoparticles. The synthesized nanoparticles of $ZnFe_2O_4$ were characterized using X-ray diffraction (XRD; Model: X'pert Pro) with Cu K_α radiation ($\lambda = 1.5406$ Å). The JCPDS PDF database was utilized for phase identification (Figure 1). Morphology and composition of the nearly pure fraction (Z5) were studied using transmission electron microscopy (TEM), scanning electron microscopy (SEM), and energy dispersive spectroscopy (EDS). Further, to confirm the composition, i.e. the stoichiometric or nonstoichiometric nature of Z5, it was annealed at 250, 350, 450 and 550 °C for 20 min and studied using XRD, Mossbauer, and vibrating sample magnetometer (VSM) techniques. Fe^{57} Mossbauer measurements were carried out in transmission mode with a $^{57}Co/Rh$ radioactive source in constant acceleration mode using a standard PC-based Mossbauer spectrometer. All Mossbauer spectra were recorded at 300 K. Magnetization measurements were conducted using a VSM at room temperature with a maximum magnetic field of 20 kG.

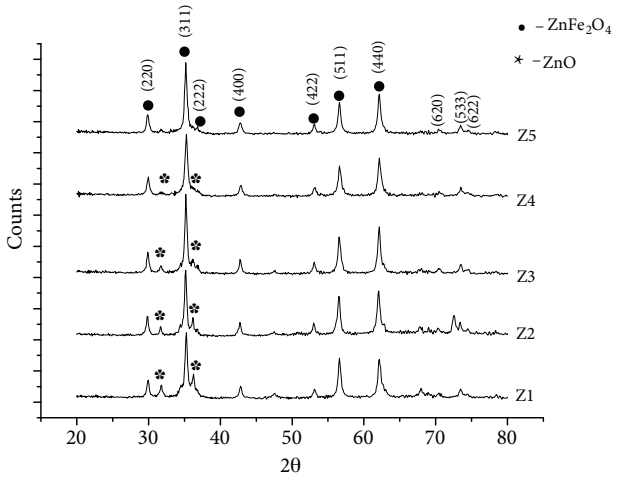

Figure 1. XRD patterns of zinc ferrite nanoparticles synthesized by varying Zn:Fe molar ratios and annealed at 450 °C.

2.2. XRD studies

The XRD patterns of the samples show well-resolved peaks, which confirm the polycrystalline and monophasic nature of the prepared material (Figure 1).

The peaks corresponding to the planes (220), (311), (222), (400), (422), (511), and (440) confirm the formation of the spinel structure of the ferrite [4,5]. However, the pyrolytic decomposition process of ferrite powders is a chemically complicated process in which many intermediate products can be formed. The phases that may be present in the sample are ZnO, Fe_2O_3, $Fe_{1-x}O$, and stoichiometric $ZnFe_2O_4$ [6]. The XRD pattern of the fractions indeed shows traces of impurity phases with varying orders. Among them, the fifth fraction (Z5) seems to be free from impure phases, and hence Z5 was chosen for further studies. The lattice parameter a of Z5, determined as 0.8447 nm, matches well with the JCPDS (89-1012) file for $ZnFe_2O_4$ (Table 1). The grain size of the zinc nanoferrite as determined using Scherrer's equation is about 20 nm. The full width at half maximum (FWHM) value of the peak corresponding to the (311) plane was chosen for calculating the particle size. It is known that the FWHM can be expressed as a linear combination of the contribution

from the lattice strain and crystalline size. The effect of strain and particle size on FWHM is expressed by the following equation:

$$\frac{\beta \cos\theta}{\lambda} = \frac{1}{\varepsilon} + \frac{\tau \sin\theta}{\theta}, \tag{1}$$

where β is the measured FWHM (in radians), θ is the Bragg angle of the peak, $\lambda$is the XRD wave length, ε is the effective particle size, and τ is the effective strain. The average particle size was determined from the extrapolation of the $\frac{\beta \cos\theta}{\lambda}$ against $\frac{\tau \sin\theta}{\theta}$ graph on the basis of the intercept inverse (Figure 2). The average particle size was found to be 20 nm. However, there is no regularity in the reported lattice parameter values. This may be attributed to the nonstoichiometric character as well as the presence of impurity phases in the samples [7]. As a bulk material, $ZnFe_2O_4$ has a normal structure, with Zn^{2+} ions occupying the tetrahedral sites and Fe^{3+} ions occupying the octahedral sites. Due to this kind of distribution, stoichiometric composition is defined at $Zn^{2+}/Fe^{3+} = 0.5$. However, when prepared as nanoparticles, a significant part of the Zn ions can enter the zinc ferrite structure at the octahedral sites, resulting in flexibility of the composition. The lattice parameters of the series of nonstoichiometric fractions (Z5–Z4) of the samples prepared in the present work change with the Zn/Fe ratio used for their synthesis. The increases in lattice parameters as well as the cell volume with increase in Zn/Fe ratio are mainly due to the larger size of the Zn^{2+} ions. However, the highly nonstoichiometric fraction (Z1) does not follow this trend, suggesting that the spinel structure is highly defective and crystallized in the mixed phase structure. The larger lattice parameter of the stoichiometric $ZnFe_2O_4$ suggests that it has a different crystal structure in terms of the distribution of the constituent cations over 2 lattice sites of the spinel structure compared to the bulk material [8].

Table 1. Structural values of zinc ferrite nanoparticles synthesized using spray pyrolysis of polymer precursor.

Sample (zinc:iron ratio)	Particle size (nm)	Lattice constant (Å) from XRD	Unit cell volume (Å^3)
Z1 (1:1)	21.5911	8.4622 ± 0.03	605.9617
Z2 (1:1.25)	21.5884	8.4882 ± 0.06	611.5731
Z3 (1:1.5)	21.5904	8.4622 ± 0.03	605.9618
Z4 (1:1.75)	21.5924	8.4240 ± 0.01	597.8074
Z5 (1:2)	20.5800	8.4475 ± 0.001	602.8158

2.3. TEM studies

The morphology and crystalline nature of the Z5 sample were investigated using TEM (Figure 3). The particles formed are fairly uniform with an average size of 15 nm. High-resolution TEM was done to confirm the findings arrived at through XRD studies.

2.4. EDS studies

The chemical composition of the $ZnFe_2O_4$ was determined using EDS. Figure 4 shows the EDS spectrum of Z5. The percentage of Zn and Fe in the sample obtained from the spectrum approximately confirms the molar ratio of 1:2 (Table 2).

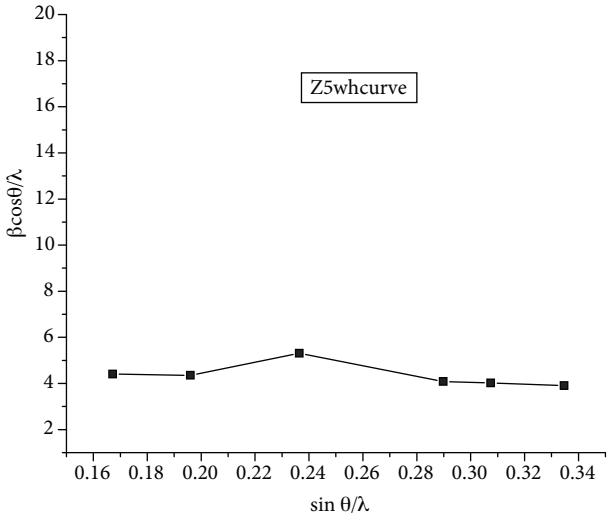

Figure 2. Williamson-Hall plot of sample Z5.

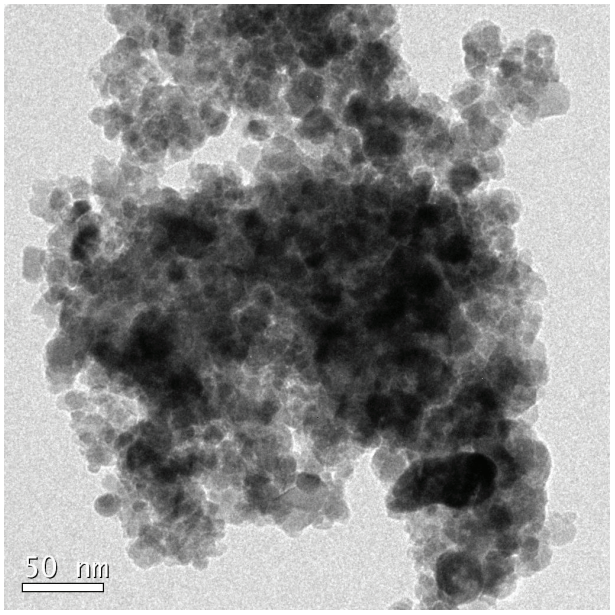

Figure 3. TEM micrograph of zinc nanoferrite particles calcined at 450 °C.

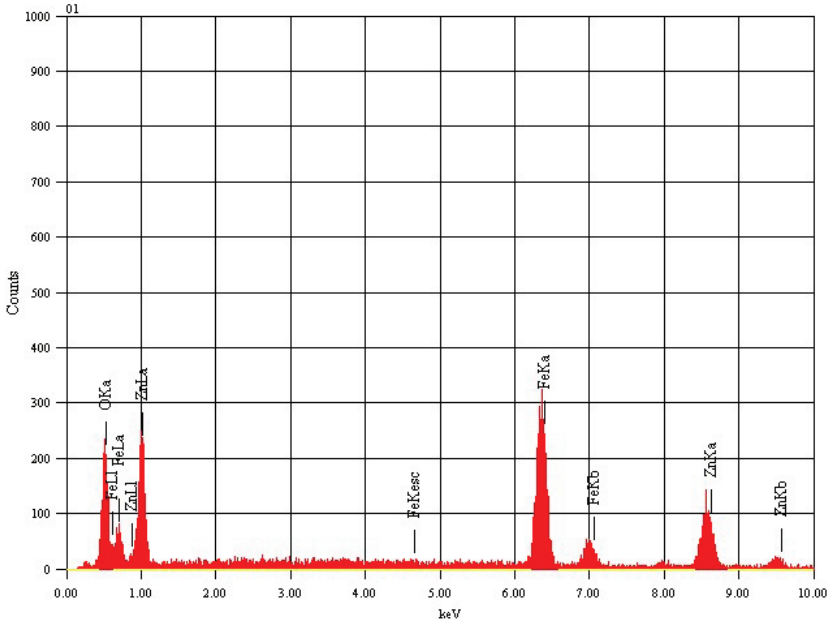

Figure 4. EDS pattern of $ZnFe_2O_4$ nanoparticles.

Table 2. The atomic abundance of elements of Z5.

Element	keV	Mass %	Atom %	K
OK	0.525	14.56	38.62	0.4247
FeK	6.398	53.30	40.51	1
ZnK	8.630	32.140	20.87	1.8766
Total		100	100	

3. Effect of annealing on particle size

3.1. XRD studies

It has been reported in the literature that annealing of ferrite nanoparticles at various temperatures and for various time periods indeed is helpful to confirm the stoichiometric character of sample. The $ZnFe_2O_4$ samples with Zn/Fe = 0.5 annealed at different temperatures are shown in Figures 5a and 5b. All the peaks in the pattern could arise from the cubic spinel structure of the sample. The average particle size and lattice parameters of the sample were estimated from the most intense peak (Table 3) [4,5]. The lattice parameters of the prepared samples are in good agreement with values reported earlier [5,6,9] and are found to be in the range of 8.4313–8.4519 Å as the annealing temperature increases from 250 to 550 °C. The data indicate that there is a gradual increase in particle size from 10.9908 to 35.5877 nm as the annealing temperature increases from 250 to 550 °C. When the nanoparticles were heated in air, their size increased, indicating that their structure was rearranged to the equilibrium bulk state. According to Makovec and Drofenik [7], Makovec et al. [8], and Nejati and Zabihi [10], the structural rearrangement at low annealing temperatures is attributed to ZnO precipitation, whereas, at high temperatures, structural rearrangement is via distribution of 2 cations between 2 spinel lattices. This process is manifested by growth of the particles. The rearrangement of cations is highly plausible because the said fraction is a highly inverted one with inversion parameter $\delta = 0.74$ determined by a low-temperature, high-field Mossbauer experiment done on the sample [11]. The presence of the ZnO phase and the growth in particle sizes with increasing annealing temperature (Figure 5; Table 3) suggest that the synthesized sample is in a 'metastable' state or a compositionally constrained state. In-depth analysis using TEM, EDS, X-ray absorption fine structure, and XRD and a series of magnetic measurements are required for confirming the status of our sample, which is not within the scope of the present work. The results further show that the pyrolysis method could be used to produce nearly pure nanosized $ZnFe_2O_4$ particles and that annealing at different temperatures provides a good means to control the particle size.

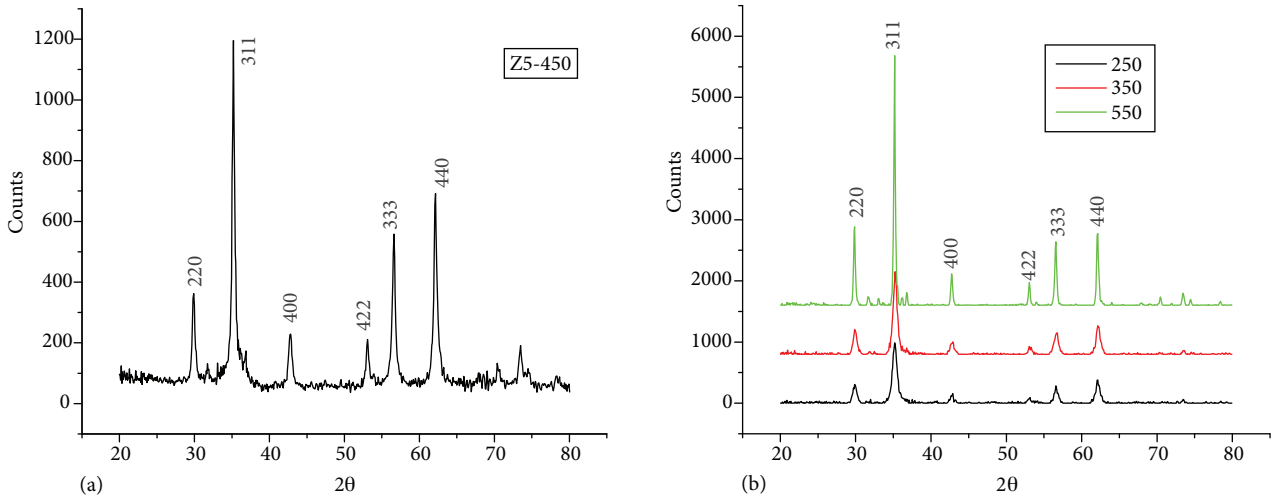

Figure 5. XRD pattern of Z5 annealed at (a) 450 and (b) 250, 350, and 550 °C.

3.2. Room-temperature Mossbauer studies

The room-temperature Fe^{57} Mossbauer spectra of all the samples shown in Figures 6a–6d are quite similar. This type of Mossbauer spectrum is common in most nanosized zinc ferrite systems, which can be attributed to

Table 3. The lattice constant and particle size of Z5 sample at different annealing temperatures.

Sample code	a (Å)	Particle size (nm)	Temperature (°C)
Z5-250	8.4462	13.1309	250
Z5-350	8.4313	10.9908	350
Z5-450	8.4485	20.7246	450
Z5-550	8.4519	35.5877	550

the superparamagnetic character [12–15]. The spectra obtained were least-square fitted and the refined values of hyperfine parameters are plotted in Figure 7 and tabulated in Table 4. Though the Mossbauer spectra of all the samples show only a doublet, there are changes in the Mossbauer parameters. In all the samples, isomer shift ranges are characteristic of Fe^{3+}. The line width of doublets in all samples is quite large. The larger widths and fluctuations in quadrupole splitting (QS) values indicate the presence of different kinds of environment around the Mossbauer probe nuclei. This may be due to the cationic exchange among ferrite sublattices of inverted spinel fraction Z5 [11]. Further, the degree of inversion, as reported by various studies, is a function of the

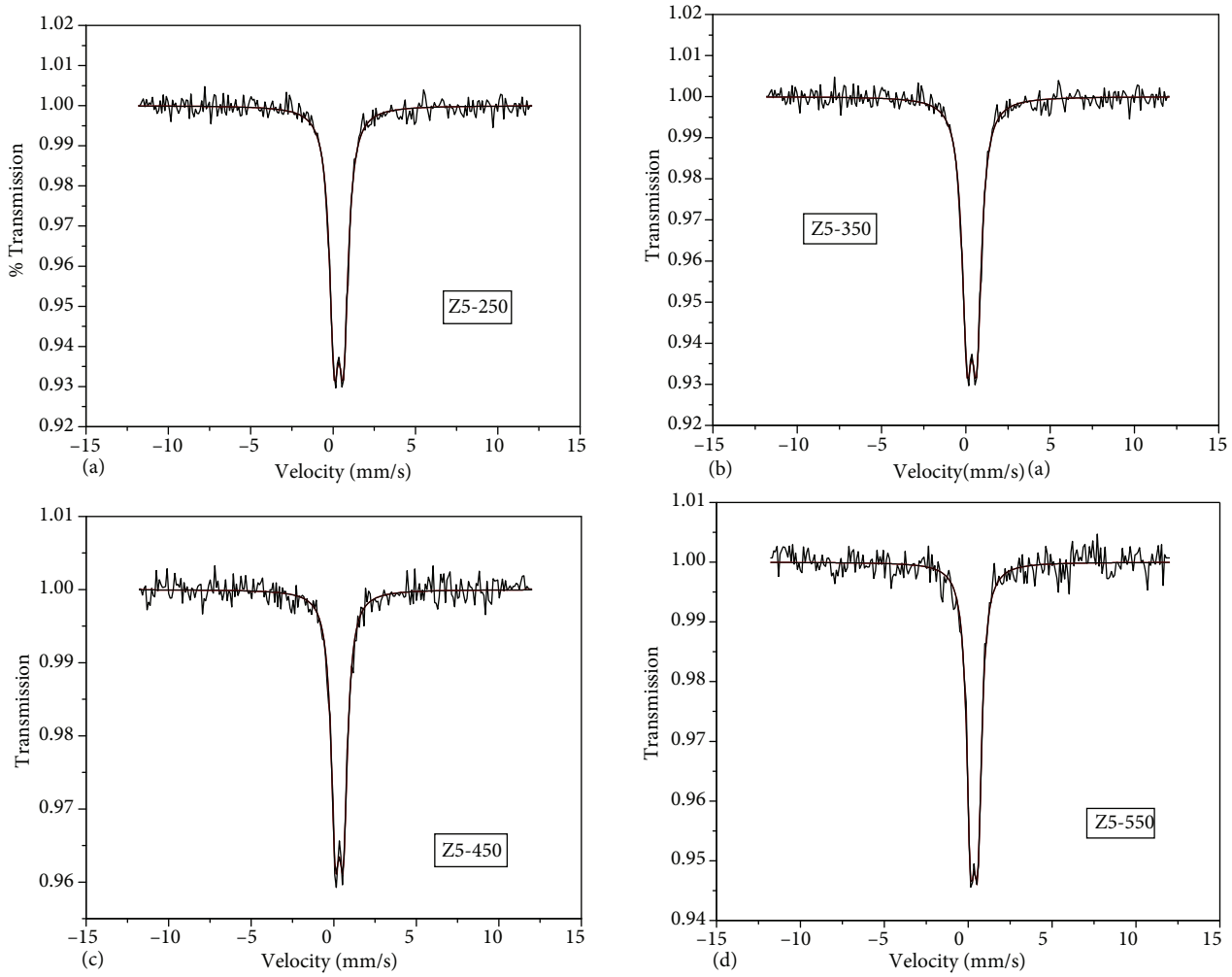

Figure 6. The Mossbauer spectra of Z5 sample at room temperature with annealing at (a) 250, (b) 350, (c) 450, and (d) 550 °C.

methods adopted in the synthesis as well as heat treatment and ball milling. For a given method, inversion decreases with heating of samples [7,8]. The fluctuations observed in the QS values also may be attributed to this factor. It has been reported that as particle sizes decrease, the Mossbauer absorption also decreases, since, in smaller particles, a larger fraction of Fe^{57} atoms will be at the surface where the crystal bonding is weak. However, this trend was not observed in our samples; instead, we observed fluctuations in recoil-free fraction values. Fluctuations in recoil-free fraction may be attributed to cation migration among lattice sites since the recoil-free fraction of Fe^{57} is different for tetrahedral and octahedral sites [9]. This fact strongly suggests that our sample is compositionally constrained and that, upon heating, cation rearrangement takes place between tetrahedral and octahedral sites.

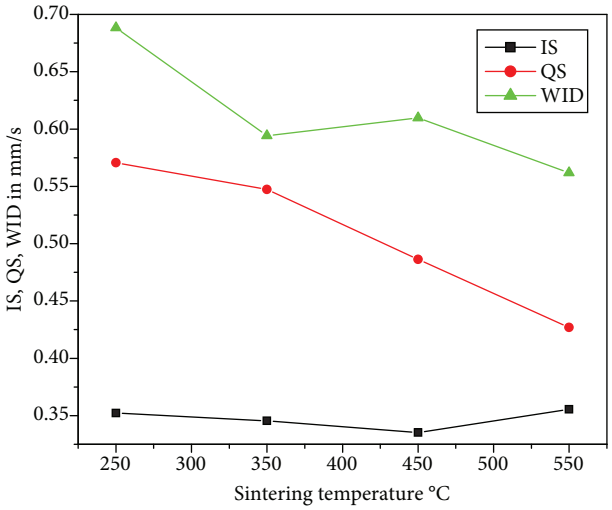

Figure 7. Mossbauer parameters [isomer shift (IS), quadrupole shift (QS), and line width (WID)] for Z5 at annealing temperatures of 250, 350, 450, and 550 °C.

Table 4. Mossbauer parameters (IS, QS, line width, area, and chi) for Z5 at sintering temperatures of 250, 350, 450, and 550 °C.

Samples at different temperature	Particle size (nm)	IS (mm/s)	QS (mm/s)	Width	Area	Chi
Z5-250	13.1309	0.3522	0.5706	0.6883	0.1164	1.0609
0.3555	35.5877	0.3555	0.4269	0.5619	0.0719	1.0625
Z5-350	10.9908	0.3454	0.5472	0.5941	0.1302	0.9021
Z5-450	20.7246	0.3352	0.4864	0.6097	0.0572	0.9296

3.3. Magnetic studies

The room temperature (300 K) magnetic properties of the zinc nanoferrites annealed at different temperatures were investigated by VSM technique in the range of –20 kOe to +20 kOe approximately. Figures 8a–8d show M-H curves for the samples. These samples show a typical S-shape in the M-H curves with varying Ms values. The variation of nanoparticles' magnetization upon annealing can be related to changes in the nanoparticles' composition due to precipitation of ZnO (reflected in the XRD patterns) and structural rearrangement between

cation sites (enhanced particle sizes) [16–18]. A careful analysis of the magnetic parameters along with particle size and structural parameters (Table 5) obtained for the fraction supports the metastable or compositionally constrained nature of the zinc ferrite nanoparticles synthesized by spray pyrolysis. Furthermore, the almost zero values of coercivity and retentivity at room temperature of these nanoparticles indicate the presence of superparamagnetism.

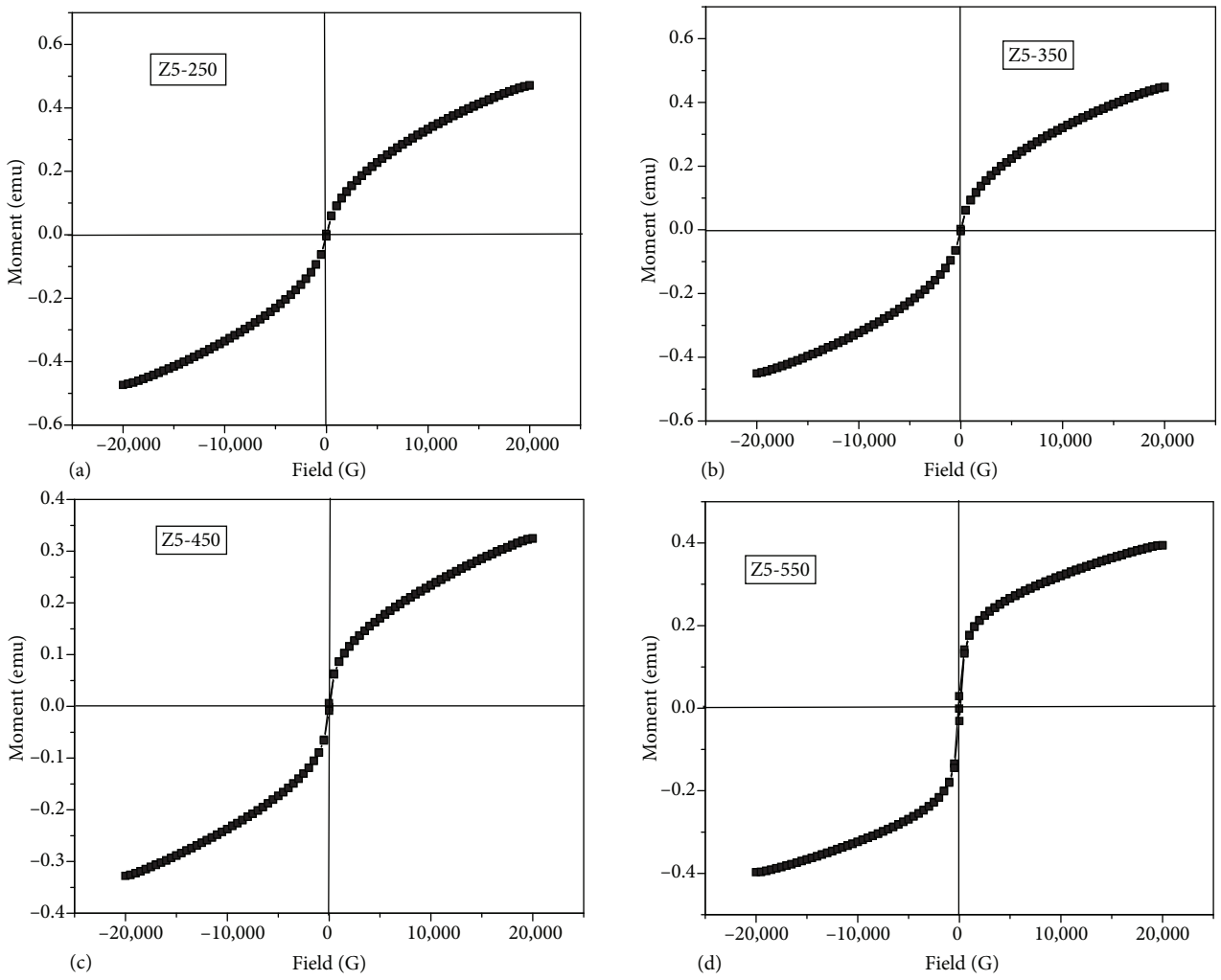

Figure 8. M-H hystersis loop of the produced Z5 at annealing temperature of (a) 250, (b) 350, (c) 450, and (d) 550 °C.

Table 5. The coercivity, retentivity, saturation magnetization per unit mass, and magnetic moment for Z5 at annealing temperatures of 250, 350, 450, and 550 °C.

	Hc (Oe)	Retentivity (emu)	Particle size (nm)	Saturation magnetization M_s (emu/g)	Magnetic moment μ_{eff} (μ_B)
Z5-250	32.5267	4.2245E-3	13.1309	9.2598	0.4000
Z5-350	27.2810	3.6011E-3	10.9908	9.1706	0.3962
Z5-450	54.0150	7.6415E-3	20.7246	7.2564	0.3135
Z5-550	92.6360	30.2740E-3	35.5877	8.0788	0.3490

4. Conclusion

Zinc ferrite spinel nanoparticles were synthesized using spray pyrolysis of polymer precursors of metal nitrates. The Zn/Fe ratio in the particles varied from 0.5 to 1. XRD patterns confirmed the formation of cubic nanocrystalline particles with particle sizes of around 20 nm, but indicated traces of ZnO and γ-Fe_2O_3 phases in all fractions. The nearly pure fraction (Zn/Fe = 0.5) was further characterized using EDS and TEM. TEM images confirmed the crystalline nature of the particles as well as the sizes of the particles, whereas EDS analysis supported the nonstoichiometric nature of the sample since the Zn/Fe ratio was found to be greater than 0.5. For confirming this nature, a temperature-dependent study was performed on the said fraction. The variations in structural parameters and particle size estimated from XRD patterns of heat-treated samples suggest that the synthesized sample is in a metastable or compositionally constrained state. The results of VSM measurements also support the said nature of the sample. Isomer shift values derived from room-temperature Mossbauer spectra of heat-treated samples were the same for all samples, which confirmed the 3+ oxidation state of iron in the sample. The presence of a doublet in all Mossbauer spectra and the negligible values of coercivity and retentivity obtained from VSM measurements for all the samples at room temperature confirmed the presence of superparamagnetism in the prepared samples.

Acknowledgments

The authors acknowledge the research grant from the University Grants Commission, New Delhi, Government of India (MRP(S)-408/08-09/ KLMG 26/UGC-SWRO, dated 30-03-09) and from the UGC-DAE Consortium for Scientific Research (CSR-1/CSR-Indore/PROS/SANC/32/2008/923. dated 04-11-08). The authors are also grateful to Prof Ajay Gupta and Dr V Raghavendra Reddy of the DAE Facilities, Indore, for providing the facilities for Mossbauer spectroscopy.

References

[1] Willard, M. A.; Kurihara, L. K.; Carpenter, E. E.; Calvin, S.; Harris, V. G. *Int. Mater. Rev.* **2004**, *49*, 125–170.

[2] Jung, D. S.; Park, S. B.; Kang, Y. C. *Korean J. Chem. Eng.* **2010**, *27*, 1621–1645.

[3] Yokoyama, M.; Sato, T.; Ohta, E. *J. Appl. Phys.* **1996**, *80*, 1015–1019.

[4] Singh, J. P.; Srivastava, R. C.; Agrawal, H. M.; Kushwaha, R. P. S. *Hyperfine Interact.* **2008**, *183*, 393–400.

[5] Cross, W. B.; Affleck, L.; Kuznetsov, M. V.; Parkin, I. P.; Pankhurst, Q. A. *J. Mater. Chem.* **1999**, *9*, 2545–2552.

[6] Yu, S.; Fujino, T.; Yoshimura, M. *J. Magn. Magn. Mater.* **2003**, *256*, 420–424.

[7] Makovec, D.; Drofenik, M. *J. Nanopart. Res.* **2008,** 10, 131–141.

[8] Makovec, D.; Kodre, A.; Arcon, I.; Drofenik, M. *J. Nanopart. Res.* **2011**, *13*, 1781–1790.

[9] Roy, M. K.; Halder, B.; Verma, H. C. *J. Korean Phys. Soc.* **2002**, *41*, 123–128.

[10] Nejati, K.; Zabihi, R. *Chem. Cent. J.* **2012**, *6*, 1–6.

[11] Jacob. J.; Vinod, V.; Mathew, J. M.; Reddy, V. R.; Abraham, K. E.; Prasad, V. S. In *ICMST Conference Proceedings: International Conference on Materials Science and Technology*, Pala, India, 10–14 June 2012.

[12] Ahn, Y.; Choi, E.; Kim, J. S. *J. Korean Phys. Soc.* **2002**, *41*, 123–128.

[13] Cullity, B. D.; Stock, S. R. *Elements of X-ray Diffraction*, 3rd ed.; Addison Wesley: Reading, MA, USA, 1956.

[14] Chinnasamy, C. N.; Narayanasamy, A.; Ponpandian, N.; Chattopadhyay, K.; Guerault, H.; Grenchheche, J. M. *J. Physics Condens. Matter* **2000**, *12*, 7795–7805.

[15] Upadhyay, C.; Verma, H. C. *Appl. Phys. Lett.* **2004**, *85*, 2074–2076.

[16] Mathew, D. S.; Juang, R. S. *Chem. Eng. Sci.* **2007**, *129*, 51–65.

[17] Singh, J. P.; Srivastava, R. C.; Agarwal, H. M.; Kumar, R. *Nucl. Instrum. Methods* **2010**, *268*, 1422–1426.

[18] Li, F. S.; Wang, L., Wang, J. B.; Zhou, Q. G.; Zhou, X. Z.; Kunkel, H. P.; Williams, G. *J. Magn. Magn. Mater.* **2004**, *268*, 332–339.